Antarctic ice-sheet meltwater reduces transient warming and climate sensitivity through the sea-surface temperature pattern effect

Yue Dong[1,2], Andrew G. Pauling[3], Shaina Sadai[4], Kyle C. Armour[3,5]

[1]Lamont-Doherty Earth Observatory, Columbia University, Palisades, NY, USA
[2]Cooperative Programs for the Advancement of Earth System Science, University Corporation for Atmospheric Research, Boulder, CO, USA
[3]Department of Atmospheric Sciences, University of Washington, Seattle, WA, USA
[4]Union of Concerned Scientists, Cambridge, MA, USA
[5]School of Oceanography, University of Washington, Seattle, WA, USA

Key Points:

- Accounting for Antarctic meltwater input in a GCM reduces the global warming rate and produces a warming pattern closer to the observed
- Antarctic meltwater impacts not only the Southern Ocean, but also the tropics via teleconnections
- The reduced global warming rate is driven by changes in both ocean heat uptake efficiency and radiative feedbacks

Corresponding author: Yue Dong, yd2644@columbia.edu

Abstract

Coupled global climate models (GCMs) generally fail to reproduce the observed sea-surface temperature (SST) trend pattern since the 1980s. The model-observation discrepancies may arise in part from the lack of realistic Antarctic ice-sheet meltwater imbalance in GCMs. Here we employ two sets of CESM1-CAM5 simulations forced by anomalous Antarctic meltwater fluxes over 1980–2013 and into the 21st century. Both show a reduced global warming rate and an SST trend pattern that better resembles observations. The meltwater drives surface cooling in the Southern Ocean and the tropical southeast Pacific, in turn increasing low-cloud cover and driving radiative feedbacks to become more stabilizing (corresponding to a lower effective climate sensitivity). These feedback changes contribute more than ocean heat uptake efficiency changes in reducing the global warming rate. Accurately projecting historical and future warming thus requires improved representation of Antarctic meltwater and its impacts in models.

Plain Language Summary

Observations have shown surface cooling in the Southern Ocean and the tropical southeast Pacific over the last four decades. However, global climate models generally struggle to reproduce this pattern. The model-observation mismatch has been proposed to partly arise from the fact that models lack in representation of realistic Antarctic ice-sheet meltwater. Here we revisit two sets of simulations with meltwater fluxes and examine the impact of meltwater input on global warming and the global energy budget. We find that accounting for meltwater input delays the global warming and produces a surface warming pattern closer to recent observations. The reduced global warming rate is caused by both more efficient ocean heat uptake and stronger radiative feedbacks (more efficient radiative damping) that are associated with changes in the surface warming pattern. These results indicate a critical impact of Antarctic meltwater on the global climate that has been missed in current climate models.

1 Introduction

The observed sea-surface temperature (SST) trend pattern since about 1979 is characterized by a strengthened west-east gradient in the tropical Pacific and a north-south hemispheric asymmetry: the tropical western Pacific and the Arctic have warmed while the tropical southeast Pacific and the Southern Ocean have cooled (England et al., 2014; Armour et al., 2016; Watanabe et al., 2021; Wills et al., 2022). The observed surface cooling in the Southern Ocean has been accompanied by an expansion of Antarctic sea ice (Fan et al., 2014; Parkinson, 2019), broad surface freshening (De Lavergne et al., 2014; Durack, 2015) and sub-surface warming (Gille, 2008; Armour et al., 2016). Yet, all these observed regional features are generally missed in global-climate model (GCM) simulations driven by historical forcings (Luo et al., 2018; Kostov et al., 2018; Chung et al., 2022; Seager et al., 2022; Wills et al., 2022; Roach et al., 2020), with many models also overestimating the global-mean warming rate over this period (Jiménez-de-la Cuesta & Mauritsen, 2019; Nijsse et al., 2020; Tokarska et al., 2020).

Various hypotheses have been put forward to explain the observed changes and model-observation discrepancies (e.g., Andrews et al., 2022). One of the leading hypotheses for the observed changes in the Southern Ocean is freshwater input from the melt of the Antarctic ice sheet and ice shelves (refereed to here as Antarctic "meltwater"). The fact that the current generation of GCMs are unable to accurately represent Antarctic meltwater imbalance may explain some of the model-observation discrepancies in the Southern Ocean. Indeed, numerous studies have shown that adding an Antarctic meltwater imbalance in GCMs can produce anomalous surface cooling, subsurface warming, and sea-ice expansion around Antarctica, owing to an increase in upper ocean stratification, reducing the vertical heat flux from the relatively warm subsurface waters below (Kirkman

& Bitz, 2011; Ma & Wu, 2011; Bintanja et al., 2013; Swart & Fyfe, 2013; Pauling et al., 2016; Armour et al., 2016; Bronselaer et al., 2018; Purich et al., 2018; Schloesser et al., 2019; Park & Latif, 2019; Sadai et al., 2020; Rye et al., 2020). Although the amount of Antarctic meltwater input needed to cause significant changes in the Southern Ocean is highly model dependent (e.g., Bintanja et al., 2013; Swart & Fyfe, 2013; Pauling et al., 2016), meltwater forcing brings projected SST trend patterns closer to those observed in all models it has been tested in.

Antarctic meltwater input may also have remote impacts, with the potential to explain some of the observed SST trends and model-observation discrepancies in the tropical Pacific. Ma and Wu (2011) demonstrated that adding anomalous Antarctic meltwater in a coupled GCM resulted in surface cooling extending from the Southern Ocean to the tropics. Hwang et al. (2017) found that enhanced Southern Ocean heat uptake in a slab-ocean model could drive a tropical La Niña-like SST response via changing the zonal-mean atmospheric heat transport. This Southern Ocean-to-tropics teleconnection has further been supported by a variety of models with anomalous zonal-mean heat fluxes in the Southern Ocean (Kang et al., 2020). More recently, Dong et al. (2022) propose a two-way atmospheric pathway associated with regional atmospheric circulation instead of zonal-mean heat transport, linking the observed cooling in the tropical eastern Pacific and the southeast Pacific sector of the Southern Ocean. Kim et al. (2022) also finds that the inter-model spread in the teleconnection between these two regions is largely determined by differences in the subtropical cloud feedback across models. All these studies suggest that the observed tropical eastern Pacific cooling may be remotely linked to the observed Southern Ocean cooling, which itself could be a direct response to Antarctic meltwater input.

Antarctic meltwater has been found to reduce projected global warming rates as well (Bronselaer et al., 2018; Schloesser et al., 2019; Sadai et al., 2020). From the standard model of global energy balance (Raper et al., 2002; Gregory & Forster, 2008; Gregory et al., 2004, 2015):

$$N = \lambda T + F = \kappa T, \tag{1}$$

the global mean near-surface air temperature trend (dT/dt) can be approximated as:

$$dT/dt = \frac{dF/dt}{\kappa - \lambda}, \tag{2}$$

where N is the global-mean energy imbalance (unit: $\mathrm{Wm^{-2}}$), F is the effective radaitive forcing (ERF; unit: $\mathrm{Wm^{-2}}$), κ is the ocean heat uptake (OHU) efficiency parameter (unit: $\mathrm{Wm^{-2}K^{-1}}$), and λ is the radiative feedback parameter (unit: $\mathrm{Wm^{-2}K^{-1}}$, negative for a stable climate). In this zero-layer energy balance model, κ and λ altogether determine the Earth's surface temperature response to an ERF, with κ representing the efficiency with which heat is absorbed by the ocean and λ representing the efficiency with which heat is radiatively emitted to space at the top of atmosphere (TOA) per degree of global warming. The reduced dT/dt found in previous meltwater simulations has been commonly proposed to arise from an increased κ, as meltwater cools the ocean surface but warms at depth, making the Southern Ocean heat uptake more efficient (Gregory, 2000; Kirkman & Bitz, 2011). However, it is also possible that meltwater reduces dT/dt by changing λ through the SST pattern effect. Recent studies have found that an SST pattern with enhanced warming in the tropical western Pacific warm pool regions and cooling in other regions, as recently observed, tends to increase the lower-tropospheric stability and low-cloud cover globally, yielding a more-negative λ and therefore a lower effective climate sensitivity (EffCS; Zhou et al., 2016; Andrews et al., 2018; Dong et al., 2019; Fueglistaler, 2019; Andrews et al., 2022). Given that Antarctic meltwater could produce surface cooling in both the Southern Ocean (due to increased ocean stratification) and the tropical eastern Pacific (due to teleconnections) – an SST pattern closer to the observed - it is possible that some portion of the reduced global warming rate is due to changes in λ via SST pattern effects. A key question is: does Antarctic meltwater primarily influence the warming rate dT/dt through changes in κ or λ?

To better understand the impact of Antarctic meltwater input on transient and near-equilibrium global warming, this study aims to quantify (i) changes in κ and λ caused by Antarctic meltwater input and (ii) the respective impacts of κ changes and λ changes on the global warming rate. To do that, we employ two sets of published simulations with additional Antarctic meltwater imbalance, the so called "hosing" simulations. One is focused on the recent historical period (leveraging simulations performed by Pauling et al. 2016); the other is focused on the 21st century (leveraging simulations performed by Sadai et al. 2020). Both studies have previously examined the local response to the imposed meltwater forcing, showing an increased Antarctic sea ice and Southern Ocean surface cooling response consistent with other studies. Here we revisit these simulations, focusing on the response of global SST patterns and the global energy budget.

2 Methods

2.1 CESM1 meltwater simulations

We analyze two sets of meltwater hosing simulations performed using the fully-coupled CESM1-CAM5 (Neale et al., 2010). The first set (from Pauling et al. 2016) spans the historical period from 1980 to 2013. We hereafter refer to these as the "Historical Hosing" runs, though the simulations apply transient historical radiative forcing until 2005 and Representative Concentration Pathway (RCP) 8.5 forcing thereafter to be consistent with CESM1 Large Ensemble (LENS) simulations (Kay et al., 2015). This ensemble consists of six members (we have performed four more since the publication of Pauling et al. 2016 following the same setup). Each of the six members has identical radiative forcing and anomalous meltwater forcing, but they are branched from a different LENS ensemble member. The anomalous freshwater input is added at a constant rate of 2000Gt/yr throughout the simulations, distributed at the front of ice shelves around Antarctica to mimic their basal melt (see Fig. 3b of Pauling et al. 2016 for the imposed freshwater distribution, with the ice shelf location derived from the RTopo-1 dataset). Note that the amount of imposed freshwater input is chosen as needed to cause significant change in the annual-mean sea ice area for CESM1 (Pauling et al. 2016) and Southern Ocean surface temperature within CESM1, which is much larger than the observational estimate of 350$\pm$100 Gt/yr (Rye et al., 2014), a caveat we will come back to in the discussion section. We present results from the ensemble-mean of the six meltwater runs, and compare changes relative to the ensemble-mean of 40 LENS runs that have no additional Antarctic meltwater (results remain the same if use the mean of the six LENS members from which the hosing runs were branched).

The other set of simulations (from Sadai et al. 2020) spans the 21st century from 2006 to 2100. We hereafter refer to these as "Future Hosing" runs. This ensemble has one control run and one meltwater hosing run; both are forced by RCP8.5 transient forcing. Although a single ensemble member, the Future Hosing run includes a large freshwater forcing, estimated by an offline ice sheet model forced by RCP8.5. The total amount of Antarctic freshwater input in the control run (from increasing precipitation only) stays around 0.1 Sv throughout the 21st century, whereas that in the hosing run (accounting for ice-sheet melting) reaches $\sim$1 Sv in 2100. Note that the total freshwater forcing applied in this simulation includes both liquid meltwater and solid ice (Fig. S1a) to account for the latent heat of melting (Fig. S1b), while in the Historical ensemble latent heat is not included. We take the difference between the control run and the meltwater run as the effect of Antarctic meltwater input in this ensemble.

2.2 Global energy budget analysis

For both Historical and Future hosing ensembles, we calculate the OHU efficiency κ and the net radiative feedback λ following the conventional global-energy budget framework expressed in Eq. (1) (Gregory et al., 2004, 2015), where $\kappa = dN/dT$, and $\lambda = d(N-F)/dT$. Note that N is taken as the global-mean net TOA radiation imbalance, which is in general equal to the global-mean OHU therefore can be used to calculate κ. One exception is the Future Hosing run, which includes the latent heat taken from the ocean to melt the solid ice. These additional heat fluxes can be accounted for by subtracting the latent heat (LH) needed to melt all the imposed solid ice from the net TOA radiation imbalance (Fig. S1), and we then calculate κ as $d(N-LH)/dT$ for this simulation. The latent heat of ice melt amounts to approximately 10% of the total global energy imbalance, and thus has a small effect on κ. Importantly, it does not influence the calculation of λ which depends only on TOA radiation. For the calculations of κ and λ, we choose to use the regression forms (over 1980–2013 for Historical Hosing and 2006–2100 for Future Hosing) since our focus is on transient warming. We also calculate the corresponding EffCS values ($= -F_{2x}/\lambda$, where F_{2x} is the radiative forcing of CO_2 doubling in CESM1), using the estimate of $F_{2x} = 3.88$ Wm^{-2} from Mitevski et al. (2021). EffCS here indicates an estimate of equilibrium climate sensitivity (ECS) using λ from a transient state, under the assumption that λ stays constant to equilibrium; it should be distinguished from the long-term Earth system sensitivity that involves changes in ice sheets operating on millennium timescales (Knutti et al., 2017).

Given that the effective radiative forcing (F) corresponding to these two ensembles is not explicitly available from CESM1 model output, we perform an additional fixed-SST simulation to estimate ERF following CMIP6 Radiative Forcing Model Intercomparison Project (RFMIP) protocol (Pincus et al., 2016). That is, we carry out a simulation using the atmospheric component of CESM1 (i.e., CAM5), with the same transient historical forcing for 1980–2013 and RCP8.5 forcing for 2006–2100 as used in the coupled CESM1 simulations, while fixing SST and sea-ice concentration at their preindustrial levels. ERF is then estimated as the TOA radiation imbalance from this fixed-SST simulation (Pincus et al., 2016; Dong et al., 2021). All variables (F, N, T) used in this study are annual means.

3 Results

3.1 Local and remote temperature responses to Antarctic meltwater input

We begin by analyzing the local response of Southern Ocean zonal-mean temperature and salinity trends (Fig. 1). In both ensembles, Antarctic meltwater input causes anomalous surface cooling, subsurface warming, and surface freshening in the Southern Ocean (Fig. 1, right column). The Future Hosing run produces stronger responses because (1) it imposes a larger amount of meltwater input and (2) it includes the effect of the latent heat of melting (which is not in the Historical ensemble). These local responses are qualitatively consistent with other studies (Bintanja et al., 2013; Bronselaer et al., 2018; Rye et al., 2020), reflecting an increase in upper ocean stratification and a decrease in upward heat transport. Moreover, accounting for meltwater produces historical temperature and salinity trends closer to observations (Fig. S2) than those simulated without meltwater input. This suggests that model-observation discrepancies in the Southern Ocean may partly arise from the models lack of ability to simulate additional meltwater due to Antarctic mass imbalance.

Next we consider the remote SST response to Antarctic meltwater input (Fig. 2). In both ensembles, the meltwater-induced Southern Ocean SST cooling extends to lower latitudes in the Southern Hemisphere (Figs. 2b, c), with the largest cooling occurring

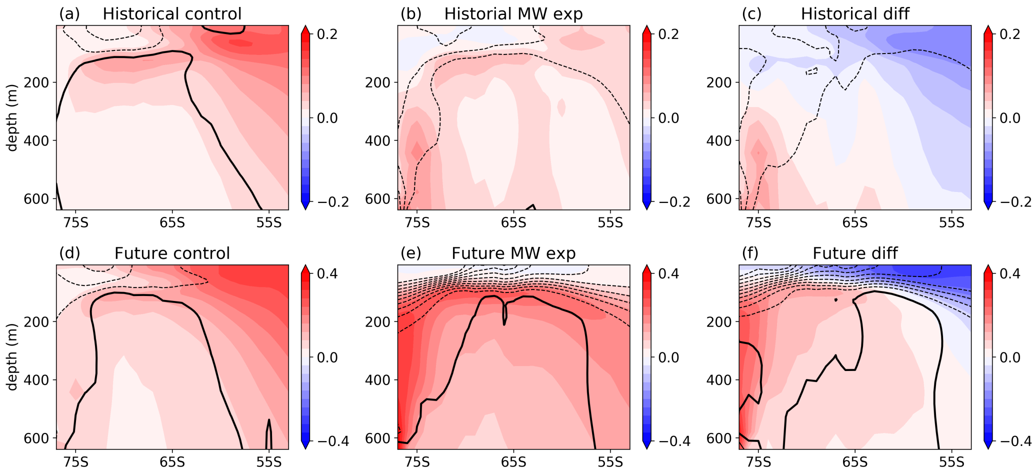

Figure 1. Zonal-mean ocean temperature trends (K/decade; shading) and salinity trends (g/kg/decade; contours) in the Southern Ocean. (a–c) Historical ensemble's control, meltwater experiment, and the difference (experiment minus control). (d–f) Future ensemble's control, meltwater experiment, and the difference. Contour interval in (a–d) is 0.01 g/kg/decade and in (e–g) is 0.02 g/kg/decade. Dashed contours denote negative anomalies; zero contours are thickened in all panels. Trends are calculated over 1980–2013 for (a–d) and 2006–2100 for (f–h).

in the eastern Pacific resulting in a La Niña-like tropical SST trend pattern (Figs. 2e, h). Notably, the Historical meltwater runs with all radiative forcings produce net cooling trends in the southeast Pacific sector of the Southern Ocean and the tropical southeast Pacific (Fig. 2d) – the two regions where observations have shown pronounced cooling trends (Fig. 2a). These two regions have also been found to have the strongest teleconnection via an atmospheric pathway, involving Rossby-wave dynamics and subtropical advection (Dong et al., 2022).

Finally, we consider how Antarctic meltwater influences the global warming rate (Fig. 3). In the Historical Hosing runs, the global-mean surface air temperature trend dT/dt (over 1980–2013) is reduced by 20%, and in the Future Hosing run dT/dt (over 2006–2100) is reduced by 28% (Table 1). Moreover, the Historical Hosing runs produce a dT/dt of 0.16 K/decade, which is more in line with the observed trend of 0.17 K/decade from HadCRUT5 (Morice et al., 2021) than that simulated without meltwater input (dT/dt = 0.2 K/decade). This suggests that the lack of Antarctic meltwater in models may explain some of the model biases in historical global-mean warming.

In summary, we find that Antarctic meltwater input in CESM1 causes local and remote climate changes that are consistent with previous studies. Accounting for anomalous meltwater input qualitatively reduces model biases in the historical record and also changes the projected warming in the near future. In the following sections we seek to further understand the relative roles of OHU efficiency κ and radiative feedback λ changes in reducing the global warming rate under meltwater forcing.

3.2 The response of κ and λ to Antarctic meltwater input

Having shown the global surface temperature response to Antarctic meltwater input, next we quantify the changes in κ and λ, two quantities that determine the change in dT/dt in a zero-layer energy balance model (Eq. 2).

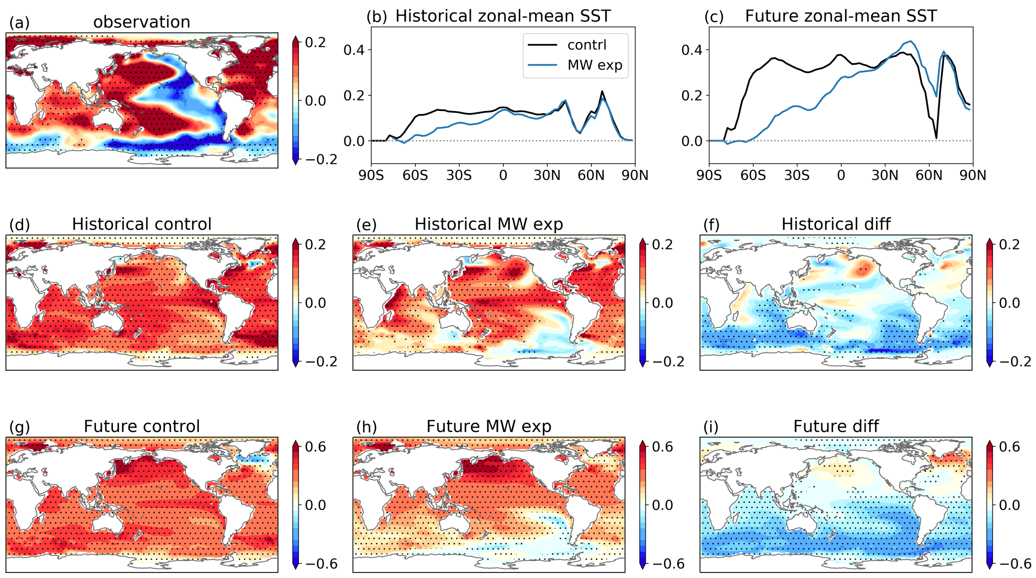

Figure 2. Global patterns of SST trends (K/decade), from (a) ERSSTv5 observation (Huang et al., 2017), (c–e) Historical control, meltwater experiment, and the difference, and (f–g) Future control, meltwater experiment, and the difference, respectively. (b–c) zonal-mean SST trends for the Historical and Future ensemble, respectively. SST trends are calculated over 1980–2013 for (a–e) and 2006–2100 for (f–h). Stippling indicates statistically significant linear trends at 95% level.

Table 1. Estimates of global-mean surface air temperature trend (dT/dt), κ, λ and EffCS for the simulations used in this study.

	Historical		Future	
	control	Meltwater	control	Meltwater
dT/dt [K/decade]	0.2	0.16	0.46	0.33
dT/dt estimated by Eq.2 [K/decade]	0.19	0.17	0.46	0.37
dT/dt_κ [K/decade]		0.18		0.43
dT/dt_λ [K/decade]		0.18		0.40
κ [$Wm^{-2}K^{-1}$]	1.15	1.28	0.5	0.62
λ [$Wm^{-2}K^{-1}$]	-1.1	-1.27	-1.01	-1.27
EffCS [K]	3.53	3.06	3.84	3.06

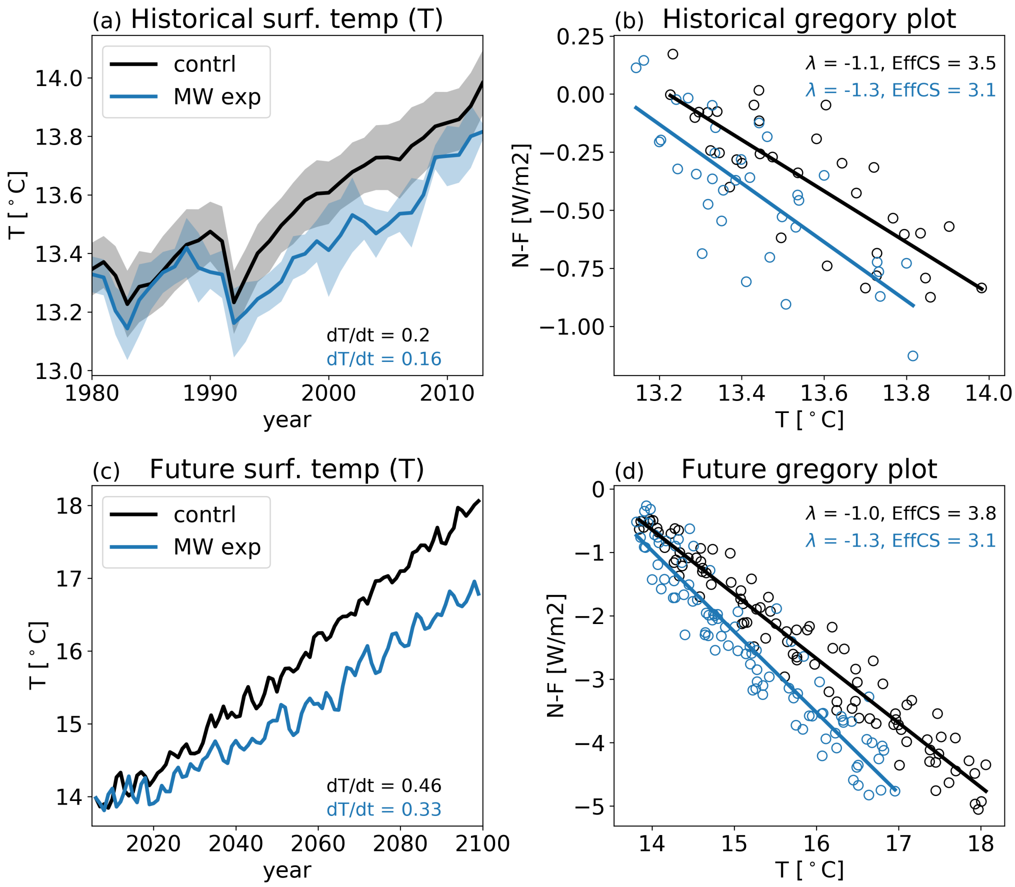

Figure 3. Ensemble-mean responses to meltwater input in (top) the Historical Hosing ensemble and (bottom) Future Hosing ensemble. (left) Global-mean surface air temperatures (T). (right) the Gregory plot (the net TOA radiative response N-F against T). Black and blue denote results of control and meltwater runs respectively. Shading in (a) represents $\pm$ one standard deviation across ensemble members.

We find that the OHU efficiency strengthens in response to Antarctic meltwater: κ increases by 11% in the Historical Hosing ensemble and by 24% in the Future Hosing run (Table 1). The strengthening of κ is not surprising given the changes in the vertical temperature distribution in the Southern Ocean shown in Fig. 1, characterized by anomalous surface cooling and subsurface warming, indicating more efficient OHU. The anomalous heat accumulation at depth has been proposed to principally arise from a reduction in upward heat transport, which is a result of either decreased isopycnic temperature gradient (Gregory, 2000; Kirkman & Bitz, 2011) and/or decreased deep ocean convection (Russell & Rind, 1999; Bintanja et al., 2013), as the upper ocean becomes more stratified.

Meanwhile, we find that the net radiative feedback also becomes more stabilizing in the meltwater runs: the magnitude of λ increases (more negative λ) by 18% in the Historical Hosing ensemble and by 30% in the Future Hosing run (Fig. 3, Table 1). Furthermore, the more-stabilizing radiative feedbacks imply lower effective climate sensitivity: EffCS is reduced from 3.5 K to 3.1 K in the Historical Hosing ensemble and from 3.8 K to 3.1 K in the Future Hosing run, values that are closer to the EffCS estimate of 2K from atmospheric model simulations forced by the osberved historical SSTs (Andrews et al., 2022). The changes in λ are primarily from the Southern Hemisphere subtropics (Fig. S3), associated with changes in the low-cloud feedback through the pattern effect (Rose et al., 2014; Rugenstein et al., 2016; Zhou et al., 2016; Dong et al., 2019). In the tropical and subtropical Pacific, the strengthened west-east SST gradient increases lower tropospheric stability, promoting more subtropical low clouds in the eastern Pacific stratocumulus deck (Wood & Bretherton, 2006; Zhou et al., 2016; Andrews et al., 2018; Dong et al., 2019). In the Southern Ocean, the meltwater-induced surface cooling locally yields a more-stable boundary layer, favoring high-coverage stratiform clouds (Dong et al., 2019; Atlas et al., 2020). In both regions, broad increases in low-cloud cover (Fig. S3) lead to stronger reflection of incoming shortwave radiation, and therefore a more-negative cloud feedback.

In summary, both κ and λ strengthen in response to Antarctic meltwater input in our simulations and thus both contribute to slowing the global warming rate. The stronger κ arises mostly from local changes in the depth of Southern Ocean heat storage. The stronger λ arises from both local (Southern Ocean) and remote (tropical) changes in cloud feedbacks owing to changes in the SST pattern.

3.3 Relative roles of κ and λ in changing the global warming rate

Finally, we come back to Eq. (2) to quantify the relative roles of κ and λ changes in reducing dT/dt. Although simplified, Eq. (2) provides an excellent approximation for the global warming rate (Gregory & Forster, 2008; Gregory et al., 2004; Andrews et al., 2022). Here, we also find that substituting values of dF/dt, κ and λ into Eq. (2) can accurately reproduce values of dT/dt from the corresponding simulations (Table 1). We can thus use the reconstructed values of dT/dt from Eq. (2), denoted as $dT/dt_{control}$ and dT/dt_{exp} for the control runs and the Hosing runs respectively, to quantify the relative contributions of changes in κ and λ.

To do so, we first estimate the value of dT/dt that would have occurred if only κ or λ changed while the other remained at the control level, denoted as dT/dt_{κ} or dT/dt_{λ}. We then calculate the change in these estimated dT/dt relative to $dT/dt_{control}$. Finally, we compare the changes in dT/dt due to changes in λ or κ alone to the total change in dT/dt (calculated as the difference between dT/dt_{exp} and $dT/dt_{control}$). We find that in the Historical Hosing ensemble, changes in κ and λ each account for approximately 50% of the total change in dT/dt; while in the Future Hosing run, κ change accounts for only 33% while λ change accounts for 67% of the total change in dT/dt (Table 1). The meltwater-induced reduction in global warming rate has long been thought to arise from more efficient OHU in the Southern Ocean (a stronger κ), our results show that Antarctic meltwater input reduces the global warming rate via changes in both OHU efficiency and radiative feedbacks. Moreover, feedback changes can produce reductions in global warming rate that are comparable to or even greater than those produced by OHU efficiency changes.

4 Conclusion and Discussion

Here we examined the impact of anomalous Antarctic meltwater on global warming and the global energy budget in two sets of CESM1-CAM5 meltwater simulations. We find that the transient global warming rate is reduced by Antarctic meltwater input, owing to both a stronger OHU efficiency and a stronger radiative feedback (corresponding to a lower effective climate sensitivity). The strengthening in κ arises mostly from local changes in the depth of Southern Ocean heat storage, while the strengthening in λ arises from both local (Southern Ocean) and remote (tropical) SST changes that enhanced negative cloud feedback through the SST pattern effect. Notably, accounting for anomalous Antarctic meltwater input produces a historical SST trend pattern better resembling observations than that simulated without meltwater input. The pattern effect-induced feedback changes contribute about equally to (in the Historical Hosing ensemble) or twice as much as (in the Future Hosing run) OHU efficiency changes in reducing the global warming rate. These findings highlight a key role of Antarctic meltwater input in modulating regional and global climates that may have been missed in current GCMs.

Our results, which are based on the use of a single GCM, come with caveats. First, the amount of additional meltwater input needed to cause significant changes in a model has been found to be highly model dependent. Here we applied an amount of Antarctic meltwater (in the Historical Hosing ensemble) to CESM1 approximately 5 to 8 times higher than observational constraints. That said, although overestimating the observed meltwater amount, our meltwater runs still underestimate the observed surface cooling and freshening over the historical period (c.f. Fig. 1b and Fig. S2). This suggests that the local and remote response to the observed Southern Ocean surface freshening in nature may be even stronger than in our simulations. Second, the extent to which κ changes in response to Antarctic meltwater input may also be model dependent. For instance, it may depend on the Southern Ocean mean state, associated with model representation of deep ocean convection (Cabré et al., 2017). Finally, while our results suggest a key role of the tropical SST pattern effect through teleconnection, the strength of the extratropical-to-tropical teleconnection appears to be also model dependent, with the inter-model spread largely coming from differences in the modeled subtropical cloud feedback (Kim et al., 2022). Thus, different results may arise from model differences in the Southern Ocean (e.g., representation of ocean mean states) and/or in the tropics (e.g., representation of atmospheric radiative feedbacks and teleconnection pathways). The robustness of our findings need to be tested in a range of models to better constrain the impact of Antarctic meltwater on global climate.

Despite these caveats, our results have important implications for understanding historical and future climate change. First, accounting for Antarctic meltwater in the Historical simulations reduces the global warming rate from 0.2 K/decade to 0.17 K/decade, which is more in line with the observational estimate of 0.16 K/decade (HadCRUT5). EffCS is also reduced from 3.5 K to 3.1 K, which is closer to the EffCS estimate of 2 K from atmospheric model simulations forced by the observed historical SST pattern (i.e., AMIP simulations) and from observed energy budget constraints (Andrews et al., 2022). Second, with realistic meltwater input, the Future Hosing run projects a muted global warming over the coming century and a lower EffCS value than those simulated without meltwater input. If our results hold in other models, this finding suggests that the near-future warming projections by current GCMs may be overestimated. Furthermore, many studies attribute the recent observed SST trend pattern (with cooling in the tropical eastern Pacific and the Southern Ocean) to internal variability (e.g., the negative phase of Inter-decadal Pacific Oscillation), and therefore hypothesize a reversed SST pattern to appear in coming decades (Watanabe et al., 2021; Chung et al., 2022). However, our simulations show that a similar historical SST pattern can arise with sufficient Antarctic meltwater forcing and that this SST pattern can persist into the 21st century in the presence of continued Antarctic meltwater input.

Additionally, several emergent constraints have been recently proposed linking model simulated historical warming to the model's equilibrium climate sensitivity (ECS). Some studies find that models with higher ECS tend to overestimate the observed global-mean warming rate over recent decades (Jiménez-de-la Cuesta & Mauritsen, 2019; Nijsse et al., 2020; Tokarska et al., 2020). Other studies find that even when models reproduce the global-mean warming, the models with too positive cloud feedback and higher ECS tend to produce less realistic interhemispheric asymmetry in surface temperatures (Wang et al., 2021). Both suggest that lower ECS values from models that better reproduce historical warming are more likely to happen. However, our simulations show that adding anomalous Antarctic meltwater can reduce model biases by producing a lower global-mean warming rate and an enhanced northern-southern hemispheric temperature asymmetry, more in line with observations (Table S1). This suggests that model biases in the transient historical warming may be (in part) due to the lack of realistic historical forcing, not necessarily due to model biases in equilibrium response to CO_2 as those emergent constraints suggested. Thus, high ECS on equilibrium timescales may be more realistic than previously thought if Antarctic meltwater input has slowed the recent southern hemispheric and global warming rates.

This work has shown a nontrivial impact of Antarctic meltwater input on climate across spatial scales (both local and global) and time scales (both transient warming and equilibrium climate sensitivity). Accurately projecting historical and future climate change thus requires improved representation of realistic Antarctic meltwater input and its impacts in GCMs.

Acknowledgments

YD was supported by the NOAA Climate and Global Change Postdoctoral Fellowship Program, administered by UCAR's Cooperative Programs for the Advancement of Earth System Science (CPAESS) under award NA210AR4310383. KCA was supported by the National Science Foundation (Grant AGS-1752796), the National Oceanic and Atmospheric Administration MAPP Program (Award NA20OAR4310391), and an Alfred P. Sloan Research Fellowship (Grant FG-2020-13568). We would like to acknowledge high-performance computing support from Cheyenne (doi:10.5065/D6RX99HX) provided by NCAR's Computational and Information Systems Laboratory, sponsored by the National Science Foundation.

Open Research

The Future Hosing simulations (first published in Sadai et al. 2020) are available at https://doi.org/10.15784/601449. The Historical Hosing ensemble (first published in Pauling et al. 2016) are available at https://doi.org/10.5281/zenodo.7072848. The CESM1 LENS simulations are obtained from https://www.cesm.ucar.edu/projects/community-projects/LENS/data-sets.

References

Andrews, T., Bodas-Salcedo, A., Gregory, J. M., Dong, Y., Armour, K. C., Paynter, D., ... others (2022). On the effect of historical SST patterns on radiative feedback. *Journal of Geophysical Research: Atmospheres*, e2022JD036675.

Andrews, T., Gregory, J. M., Paynter, D., Silvers, L. G., Zhou, C., Mauritsen, T., et al. (2018). Accounting for changing temperature patterns increases historical estimates of climate sensitivity. *Geophysical Research Letters*, *45*(16), 8490–8499.

Armour, K. C., Marshall, J., Scott, J. R., Donohoe, A., & Newsom, E. R. (2016). Southern Ocean warming delayed by circumpolar upwelling and equatorward transport. *Nature Geoscience*, *9*(7), 549–554.

Atlas, R., Bretherton, C. S., Blossey, P. N., Gettelman, A., Bardeen, C., Lin, P., & Ming, Y. (2020). How well do large-eddy simulations and global climate models represent observed boundary layer structures and low clouds over the summertime southern ocean? *Journal of Advances in Modeling Earth Systems*, *12*(11), e2020MS002205.

Bintanja, R., van Oldenborgh, G. J., Drijfhout, S., Wouters, B., & Katsman, C. (2013). Important role for ocean warming and increased ice-shelf melt in Antarctic sea-ice expansion. *Nature Geoscience*, *6*(5), 376–379.

Bronselaer, B., Winton, M., Griffies, S. M., Hurlin, W. J., Rodgers, K. B., Sergienko, O. V., ... Russell, J. L. (2018). Change in future climate due to Antarctic meltwater. *Nature*, *564*(7734), 53–58.

Cabré, A., Marinov, I., & Gnanadesikan, A. (2017). Global atmospheric teleconnections and multidecadal climate oscillations driven by Southern Ocean convection. *Journal of Climate*, *30*(20), 8107–8126.

Chung, E.-S., Kim, S.-J., Timmermann, A., Ha, K.-J., Lee, S.-K., Stuecker, M. F., et al. (2022). Antarctic sea-ice expansion and Southern Ocean cooling linked to tropical variability. *Nature Climate Change*, *12*(5), 461–468.

De Lavergne, C., Palter, J. B., Galbraith, E. D., Bernardello, R., & Marinov, I. (2014). Cessation of deep convection in the open Southern Ocean under anthropogenic climate change. *Nature Climate Change*, *4*(4), 278–282.

Dong, Y., Armour, K. C., Battisti, D. S., & Blanchard-Wrigglesworth, E. (2022). Two-way teleconnections between the Southern Ocean and the tropical Pacific via a dynamic feedback. *Journal of Climate*, 1–37.

Dong, Y., Armour, K. C., Proistosescu, C., Andrews, T., Battisti, D. S., Forster, P. M., et al. (2021). Biased estimates of equilibrium climate sensitivity and transient climate response derived from historical CMIP6 simulations. *Geophysical Research Letters*, *48*(24), e2021GL095778.

Dong, Y., Proistosescu, C., Armour, K. C., & Battisti, D. S. (2019). Attributing historical and future evolution of radiative feedbacks to regional warming patterns using a Green's function approach: The preeminence of the western Pacific. *Journal of Climate*, *32*(17), 5471–5491.

Durack, P. J. (2015). Ocean salinity and the global water cycle. *Oceanography*, *28*(1), 20–31.

England, M. H., McGregor, S., Spence, P., Meehl, G. A., Timmermann, A., Cai, W., et al. (2014). Recent intensification of wind-driven circulation in the Pacific and the ongoing warming hiatus. *Nature climate change*, *4*(3), 222–227.

Fan, T., Deser, C., & Schneider, D. P. (2014). Recent Antarctic sea ice trends in the context of Southern Ocean surface climate variations since 1950. *Geophysical Research Letters*, *41*(7), 2419–2426.

Fueglistaler, S. (2019). Observational evidence for two modes of coupling between sea surface temperatures, tropospheric temperature profile, and shortwave cloud radiative effect in the tropics. *Geophysical Research Letters*, *46*(16), 9890–9898.

Gille, S. T. (2008). Decadal-scale temperature trends in the Southern Hemisphere ocean. *Journal of Climate*, *21*(18), 4749–4765.

Gregory, J. M. (2000). Vertical heat transports in the ocean and their effect on time-dependent climate change. *Climate Dynamics*, *16*(7), 501–515.

Gregory, J. M., Andrews, T., & Good, P. (2015). The inconstancy of the transient climate response parameter under increasing CO_2. *Philosophical Transactions of the Royal Society A: Mathematical, Physical and Engineering Sciences*, *373*(2054), 20140417.

Gregory, J. M., & Forster, P. (2008). Transient climate response estimated from radiative forcing and observed temperature change. *Journal of Geophysical Research: Atmospheres*, *113*(D23).

Gregory, J. M., Ingram, W. J., Palmer, M. A., Jones, G. S., Stott, P. A., Thorpe, R. B., et al. (2004). A new method for diagnosing radiative forcing and climate sensitivity. *Geophysical research letters*, *31*(3).

Huang, B., Thorne, P. W., Banzon, V. F., Boyer, T., Chepurin, G., Lawrimore, J. H., ... Zhang, H.-M. (2017). Extended reconstructed sea surface temperature, version 5 (ERSSTv5): upgrades, validations, and intercomparisons. *Journal of Climate*, *30*(20), 8179–8205.

Hwang, Y.-T., Xie, S.-P., Deser, C., & Kang, S. M. (2017). Connecting tropical climate change with southern ocean heat uptake. *Geophysical Research Letters*, *44*(18), 9449–9457.

Jiménez-de-la Cuesta, D., & Mauritsen, T. (2019). Emergent constraints on Earth's transient and equilibrium response to doubled CO_2 from post-1970s global warming. *Nature Geoscience*, *12*(11), 902–905.

Kang, S. M., Xie, S.-P., Shin, Y., Kim, H., Hwang, Y.-T., Stuecker, M. F., et al. (2020). Walker circulation response to extratropical radiative forcing. *Science advances*, *6*(47), eabd3021.

Kay, J. E., Deser, C., Phillips, A., Mai, A., Hannay, C., Strand, G., ... others (2015). The Community Earth System Model (CESM) large ensemble project: A community resource for studying climate change in the presence of internal climate variability. *Bulletin of the American Meteorological Society*, *96*(8), 1333–1349.

Kim, H., Kang, S. M., Kay, J. E., & Xie, S.-P. (2022). Subtropical clouds key to Southern Ocean teleconnections to the tropical pacific. *Proceedings of the National Academy of Sciences*, *119*(34), e2200514119.

Kirkman, C. H., & Bitz, C. M. (2011). The effect of the sea ice freshwater flux on Southern Ocean temperatures in CCSM3: Deep-ocean warming and delayed surface warming. *Journal of Climate*, *24*(9), 2224–2237.

Knutti, R., Rugenstein, M. A., & Hegerl, G. C. (2017). Beyond equilibrium climate sensitivity. *Nature Geoscience*, *10*(10), 727–736.

Kostov, Y., Ferreira, D., Armour, K. C., & Marshall, J. (2018). Contributions of greenhouse gas forcing and the southern annular mode to historical southern ocean surface temperature trends. *Geophysical Research Letters*, *45*(2), 1086–1097.

Luo, J.-J., Wang, G., & Dommenget, D. (2018). May common model biases reduce CMIP5's ability to simulate the recent Pacific la niña-like cooling? *Climate Dynamics*, *50*(3), 1335–1351.

Ma, H., & Wu, L. (2011). Global teleconnections in response to freshening over the Antarctic ocean. *Journal of climate*, *24*(4), 1071–1088.

Mitevski, I., Orbe, C., Chemke, R., Nazarenko, L., & Polvani, L. M. (2021). Non-monotonic response of the climate system to abrupt CO_2 forcing. *Geophysical research letters*, *48*(6), e2020GL090861.

Morice, C. P., Kennedy, J. J., Rayner, N. A., Winn, J., Hogan, E., Killick, R., ... Simpson, I. (2021). An updated assessment of near-surface temperature change from 1850: the HADCRUT5 data set. *Journal of Geophysical Research: Atmospheres*, *126*(3), e2019JD032361.

Neale, R. B., Chen, C.-C., Gettelman, A., Lauritzen, P. H., Park, S., Williamson, D. L., ... others (2010). Description of the NCAR community atmosphere model (CAM 5.0). *NCAR Tech. Note NCAR/TN-486+ STR*, *1*(1), 1–12.

Nijsse, F. J., Cox, P. M., & Williamson, M. S. (2020). Emergent constraints on transient climate response (TCR) and equilibrium climate sensitivity (ECS) from historical warming in CMIP5 and CMIP6 models. *Earth System Dynamics*, *11*(3), 737–750.

Park, W., & Latif, M. (2019). Ensemble global warming simulations with idealized Antarctic meltwater input. *Climate Dynamics*, *52*(5), 3223–3239.

Parkinson, C. L. (2019). A 40-y record reveals gradual Antarctic sea ice increases followed by decreases at rates far exceeding the rates seen in the Arctic. *Proceedings of the National Academy of Sciences*, *116*(29), 14414–14423.

Pauling, A. G., Bitz, C. M., Smith, I. J., & Langhorne, P. J. (2016). The response of the Southern Ocean and Antarctic sea ice to freshwater from ice shelves in an Earth system model. *Journal of Climate*, *29*(5), 1655–1672.

Pincus, R., Forster, P. M., & Stevens, B. (2016). The Radiative Forcing Model Intercomparison Project (RFMIP): experimental protocol for CMIP6. *Geoscientific Model Development*, *9*(9), 3447–3460.

Purich, A., England, M. H., Cai, W., Sullivan, A., & Durack, P. J. (2018). Impacts of broad-scale surface freshening of the Southern Ocean in a coupled climate model. *Journal of Climate*, *31*(7), 2613–2632.

Raper, S. C., Gregory, J. M., & Stouffer, R. J. (2002). The role of climate sensitivity and ocean heat uptake on AOGCM transient temperature response. *Journal of Climate*, *15*(1), 124–130.

Roach, L. A., Dörr, J., Holmes, C. R., Massonnet, F., Blockley, E. W., Notz, D., ... others (2020). Antarctic sea ice area in CMIP6. *Geophysical Research Letters*, *47*(9), e2019GL086729.

Rose, B. E., Armour, K. C., Battisti, D. S., Feldl, N., & Koll, D. D. (2014). The dependence of transient climate sensitivity and radiative feedbacks on the spatial pattern of ocean heat uptake. *Geophysical Research Letters*, *41*(3), 1071–1078.

Rugenstein, M. A., Caldeira, K., & Knutti, R. (2016). Dependence of global radiative feedbacks on evolving patterns of surface heat fluxes. *Geophysical Research Letters*, *43*(18), 9877–9885.

Russell, G. L., & Rind, D. (1999). Response to CO_2 transient increase in the GISS coupled model: regional coolings in a warming climate. *Journal of Climate*, *12*(2), 531–539.

Rye, C. D., Marshall, J., Kelley, M., Russell, G., Nazarenko, L. S., Kostov, Y., ... Hansen, J. (2020). Antarctic glacial melt as a driver of recent Southern Ocean climate trends. *Geophysical Research Letters*, *47*(11), e2019GL086892.

Rye, C. D., Naveira Garabato, A. C., Holland, P. R., Meredith, M. P., George Nurser, A., Hughes, C. W., et al. (2014). Rapid sea-level rise along the Antarctic margins in response to increased glacial discharge. *Nature Geoscience*, *7*(10), 732–735.

Sadai, S., Condron, A., DeConto, R., & Pollard, D. (2020). Future climate response to Antarctic Ice Sheet melt caused by anthropogenic warming. *Science advances*, *6*(39), eaaz1169.

Schloesser, F., Friedrich, T., Timmermann, A., DeConto, R. M., & Pollard, D. (2019). Antarctic iceberg impacts on future Southern Hemisphere climate. *Nature Climate Change*, *9*(9), 672–677.

Seager, R., Henderson, N., & Cane, M. (2022). Persistent discrepancies between observed and modeled trends in the tropical Pacific Ocean. *Journal of Climate*, 1–41.

Swart, N., & Fyfe, J. (2013). The influence of recent Antarctic ice sheet retreat on simulated sea ice area trends. *Geophysical Research Letters*, *40*(16), 4328–4332.

Tokarska, K. B., Stolpe, M. B., Sippel, S., Fischer, E. M., Smith, C. J., Lehner, F., & Knutti, R. (2020). Past warming trend constrains future warming in CMIP6 models. *Science advances*, *6*(12), eaaz9549.

Wang, C., Soden, B. J., Yang, W., & Vecchi, G. A. (2021). Compensation between cloud feedback and aerosol-cloud interaction in CMIP6 models. *Geophysical research letters*, *48*(4), e2020GL091024.

Watanabe, M., Dufresne, J.-L., Kosaka, Y., Mauritsen, T., & Tatebe, H. (2021). Enhanced warming constrained by past trends in equatorial Pacific sea surface temperature gradient. *Nature Climate Change*, *11*(1), 33–37.

Wills, R. C. J., Dong, Y., Proistosecu, C., Armour, K. C., & Battisti, D. S. (2022). Systematic climate model biases in the large-scale patterns of recent sea-surface temperature and sea-level pressure change. *Geophysical Research Letters*, *49*(17), e2022GL100011.

Wood, R., & Bretherton, C. S. (2006). On the relationship between stratiform low cloud cover and lower-tropospheric stability. *Journal of climate*, *19*(24), 6425–6432.

Zhou, C., Zelinka, M. D., & Klein, S. A. (2016). Impact of decadal cloud variations on the Earth's energy budget. *Nature Geoscience*, *9*(12), 871–874.